ANNALS of Faculty Engineering Hunedoara – International Journal of Engineering
Tome XX [2022] | Fascicule 4 [November]

[1,2]Tienah H. H. ELAGIB, [1]Nassereldeen A. KABBASHI, [2]Elwathig A.M. HASSAN, [1]Md. Zahangir ALAM, [1]Ma'an F. Al–KHATIB

THE ROLE OF HIGH–PERFORMANCE MICROWAVE ABSORBING MATERIALS IN ELECTROMAGNETIC INTERFERENCE SHIELDING: A REVIEW OF THE ADVANCED INTERNAL DESIGN OF POLYMER–BASED NANO–COMPOSITES

[1] Faculty of Engineering, International Islamic University Malaysia, Gombak 53100, Kuala Lumpur, MALAYSIA
[2] Faculty of Industrial Engineering and Technology, University of Gezira, Wad Madani, Gezira State, SUDAN

Abstract: Electromagnetic interference (EMI) shielding refers to the ability of a material to block the EM waves generated by electronic systems. In the past few decades, there has been sustained research in the use of conductive metal and conductive polymer–based shielding approaches, but these have shown difficulties with high density and processability. In recent years, other strategies have been developed to obtain more practical shielding materials. A summary of lightweight polymer–based nanocomposites with EM absorption characteristics for EMI shielding is provided. The advantages, disadvantages, and EMI shielding mechanisms of various types of nanocomposites are discussed. This article focused on understanding the approaches related to different types of fillers, which include carbon materials as well as metal particles and microwires which are used separately and in the form of hybrids designed to achieve highly effective shielding capabilities. This review focuses on structure configurations such as multilayer structures, coating, and advanced three–dimensional (3D) structures, which may be used to encourage the development of more environmentally responsible EMI shielding materials. In summary, it can be said that the thickness, dielectric, magnetic characteristics, and filler concentration, can be adjusted to obtain the desired combination of higher shielding performance and EM absorption properties.
Keywords: electromagnetic interference; shielding efficiency; electrical conductivity; conductive network; microwave absorption

1. INTRODUCTION

Electromagnetic interference (EMI) has become an inescapable hazard due to the rapid progress of communications technologies and deeply integrated electronic equipment, as well as the demand to establish precise signal transmission networks, which considerably impairs the proper operation of the electronics around it, the human health[1, 2], biological systems, and defense–oriented applications when exposed [3–5], as it causes many forms of cancers such as brain tumors, [6] leukemia [7], and breast cancer [8]. Furthermore, such electronic components suffer from the accumulation of unwanted thermal energy [9], which reduces their performance and durability [4]. Since this can have serious consequences, it is imperative to study these claims better. Therefore, to filter the receiving and outgoing disturbances protective shields are essential to eliminate EMI for the simultaneous hassle–free operation of many devices[10].

The employment of magnetic or conductive materials to restrict the propagation of electric and magnetic waves from one point to another is known as EMI shielding. This shielding can be created by limiting the quantity of signal that flows through a system, either through reflection or wave absorption [11].

Because of the rapid advancement of electronic communication technology, like the recently deployed fifth–generation (5G) mobile network communication techniques, data transfer speeds have reached previously unheard–of levels [12]. As a result, creating high–performance EMI shielding materials has become a pressing need in order to address the increasing demands for EM radiation protection [13].

The production of EMI–shielded materials has recently acquired popularity in both academic and industry circles. Active study and numerous techniques in this regard have been undertaken, including the design of diverse material shapes. Shielding material should be electrically conducting and dielectrically and/or magnetically lossy [14], (i.e. it can reduce EM waves through electrical, magnetic, and dielectric loss) [15].

The traditional approach to EMI shielding depends on the use of metallic materials that have high blocking capability [16]. In particular, typical metals such as aluminum and copper are excessively used, due to their high conductivity (σ) and dielectric constant (ε) which contribute to high EM1 shielding efficiency (SE). Although typical metals have great shielding performance, their poor processability, high–density [17] corrosion, costly processing, and high surface reflection drawbacks [18], have severely hampered their promotion and wider deployment [19], particularly in next generation portable devices, wearable electronics, and automobiles [20].

Recent research has focused on the production of lightweight EMI shielding materials with high SE [21–23]. Because of their conductivity, intrinsically conducting polymers (ICP) are frequently used in a wide range of electrical applications. Polyaniline, in particular, is being explored for EMI shielding to replace corrosive and dense metals due to its environmental stability, ease of polymerization, low cost, chemical and environmental stability [8], high conductivity, and low density [24]. Despite the fact that ICPs can be used with or without filler for shielding, they exhibit poor processability and mechanical properties [25].

Polymers, on the other hand, have multiple advantageous qualities such as lightweight, simplicity of processing, and high corrosion resistivity. However, due to restrictions such as low electrical conductivity, polymers are useless when compared to metals [26]. In this manner, two approaches are used to improve their electrical conductivity and EMI shielding capability: coating with conductive materials or combining with conductive materials to produce nanocomposites [27].

Polymer–based nanocomposites are projected to be more promising EMI shielding materials due to their unique combination of electrical conductivity and polymer flexibility, low weight, ease of processing, cheap cost, corrosion resistance, and tunable characteristics with excellent shielding capabilities [27–30]. Several nanocomposites have been created for EMI shielding, with an emphasis on generic polymers (e.g., polystyrene [31], polyethylene [32], polypropylene [33, 34]), engineering polymers (e.g., polyamide [35], polyethylene terephthalate [36], polycarbonate [37]), and non–petroleum based polymers (e.g., polylactic acid [38], polycaprolactone [39]). According to our knowledge, superior SE with light weight and strong heat resistance are highly demanded for practical applications of EMI shielding materials in fields such as automobiles, aerospace, and aircraft [40].

Carbon–based materials such as CFs [41], Carbon black [42], carbon nano–fibers [43, 44], especially, graphene [45, 46] and carbon nanotubes (CNTs) [42, 46–48] have been employed as fillers and combined with polymers to create nanocomposites for EMI shielding due to their high electrical conductivity, excellent mechanical properties, lightweight, and high aspect ratio [49]. Graphene, in particular, is a rising star material with a plethora of attractive characteristics like high specific surface area, outstanding electrical conductivity, excellent thermal conductivity, light weight, high intrinsic mobility, excellent mechanical stiffness, high Young's modulus, and optical transmittance [5]. In general, due to their confined electron–strong interaction in a plane, significant anisotropy, and quantum effect, two–dimensional (2D) nano–sheets frequently exhibit unusual electrical behavior, large specific surface area, and low mass density. Furthermore, because nano–sheets can be easily produced into high–orientation multilayered composites, they can operate as an effective barrier to energy waves by lengthening the propagation route [50]. However, the small lateral dimension of graphene flakes, which hinders efficient stress transfer from the surrounding matrix, the challenges with particle dispersion, and the limited control of flake thickness are all characteristics of discontinuous graphene composites. As a result, substantial filler loadings are typically required to achieve adequate electrical and thermal conductivities as well as modest SE [51]. On the other hand, magnetic nanomaterials, such as nanowires [14] and silver (Ag) nanoparticles (NPs) [52], as well as 'hexa–ferrite, spinel–ferrite, Fe, Ni, and Co NPs' and their alloys [50], have enhanced the potential advancement of polymer nanocomposites, particularly when combined with carbonaceous materials [24]. Magnetic dipoles in these magnetic NPs interact with the magnetic field related with the receiving EM waves. In addition, the increased permeability of these magnetic NPs contributes to decreasing the impedance of the nanocomposite [53].

This contribution discusses the concept of electromagnetic interference (EMI) and the shielding mechanisms for that interference and hopes it can serve as a starting point for students and researchers in chemical engineering and materials science. This article is designed to provide a summary of the literature as well as specifics, in part, on several materials with diverse designs and fabrication strategies for EMI blocking. Although numerous materials' shielding performance has been extensively explored, the focus of this paper is on the different internal structures of polymer–based nanocomposites.

2. EMI SHIELDING MECHANISM

The EMWs be consist of oscillating magnetic (H) and electric (E) fields (see Figure 1) that move with the same phase at a certain point in time. The electric field is blocked by all conductive materials depending on the intensity of the charge, while the magnetic field, determined by the movement of the charges, penetrates all materials. Magnetic fields, in particular, are considered more harmful to health than electric fields [54]. According to the World Health Organization (Who), the potential risk to human health increases with exposure to higher EM waves; Exposures at higher levels of 100 kHz to 300 GHz, which could be harmful, are restricted by national and international guidelines [55, 56].

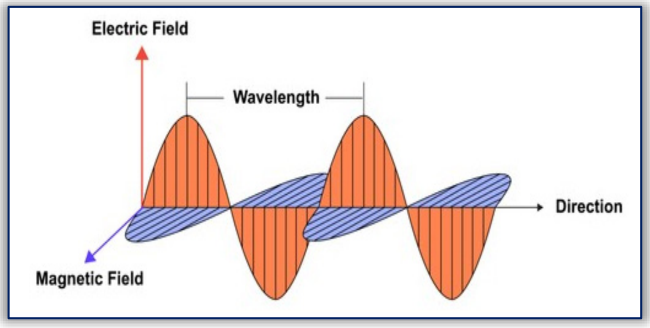

Figure 1– Schematic displaying the vector of EM radiation (permission granted by the publisher) [57].

The relative magnitude relies on the shape of the wave source. The ratio of E to H is called the wave impedance 'the inherent impedance of the free space is 377 Ω'. Large impedances differentiate electric fields, small ones differentiate magnetic fields. In addition, the EMI shielding consists of two zones, the near–field, and the far–field zone. If the distance between the shield and the radiation source is greater than $\lambda/2\pi$ (where λ is the wavelength of the radiation source), is in the far–field shielding zone. The EM plane wave theory is usually applied for EMI shielding in this area. When the distance is lower than $\lambda/2\pi$, it is in the near field shielding, therefore, the theory based on the contribution of electric and magnetic dipoles is used for EMI shielding [57, 58].

The performance of shielding material is usually expressed in terms of shielding effectiveness (SE), expressed in decibels (dB). SE can be defined as the logarithmic ratio of the incident radiation (P_I) and the transmitted (P_T) power of an EM wave that passing through a material [59] and is given by Eq. 1;

$$10\ \log\left|\frac{P_I}{P_T}\right| = 20\ \log\left|\frac{E_I}{E_T}\right| = 20\ \log\left|\frac{H_I}{H_T}\right| \quad (1)$$

where P, E, and H represent the field intensity of plane–wave, electric, and magnetic field intensities, respectively.

According to Schelkunoffs theory, three mechanisms have been reported that contribute to the overall EMI shielding effectiveness (SE_T) of a material; namely reflection (R), absorption (A), and multiple–reflections (the internal reflections within the shielding material) [60, 61].

Shielding effectiveness (SE) is a logarithmic quantity and can be expressed as the sum of SE (Eq.2) due to reflection (SE_R), absorption (SE_A), and multiple reflections (SE_M) [62]:

$$SE_T = SE_R + SE_A + SE_M, \quad (2)$$

It is documented that the materials with SE greater than 20 dB can meet the general civil requirements. However, aerospace and defense–oriented electronic equipment require an SE greater than 30 dB, and some precision instruments even higher [63]. In fact, the thickness of the shielding material, its intrinsic EM characteristics, and the frequency of the EM radiation all influence SE_T [64].

In the case of homogeneous conductive shielding material (not a composite of a conductive filler and insulating polymer) reflection is generally the primary shielding mechanism. For shielding by reflection, the material must have movable charge carriers (electrons or holes) to be able to interact with the incident EM waves [64, 65]. The reflection of incident waves can also depend on the relative mismatch between the incident wave and the surface impedance of the shield [62], which is correlated with the material conductivity. If the magnitude of the wave impedance is differing significantly from the intrinsic impedance of the shielding material, most of the EM wave will be reflected and very little will be transmitted across the boundary. Highly dielectric materials induce more reflection than absorption, while materials with high permeability are better suited for absorption [66]. In addition, the wave reflections resulting from high conductivity lead to EM secondary pollution [67].

A secondary mechanism of EMI shielding is usually absorption. The absorption characteristics rely on the frequency, dielectric permittivity, magnetic permeability, and thickness [68]. In addition, the performance of shielding through absorption increases with the presence of electrical and/ or magnetic dipoles in the shield that can interact with the EM radiation. EMI shielding is only considered for the dielectric properties when the magnetic properties are absent, and the opposite is true [59].

Once the RL of an EM absorber is less than −10 dB, roughly 10% of the EM energy is reflected and 90% is absorbed. The corresponding frequency range where the RC is less than −10 dB is denoted as the effective absorption bandwidth (EAB). EM absorbing materials are predicted to have a thin thickness, lightweight, and inexpensive cost in addition to a minimal RL and a wide EAB [69].

EM absorbing materials can be a more practical substitute for traditional reflective–based shields by converting EM energy into thermal energy and dissipating it through the surface. The combination of magneto–dielectric loss and conductivity must be taken into account to obtain an acceptable SE [70]. For example, conductive fillers like graphene can be doped with nitrogen through hydrothermal and thermal annealing to modulate their electrical and magnetic characteristics, creating light absorbers with perfect EM matching without the addition of magnetic fillers [71]

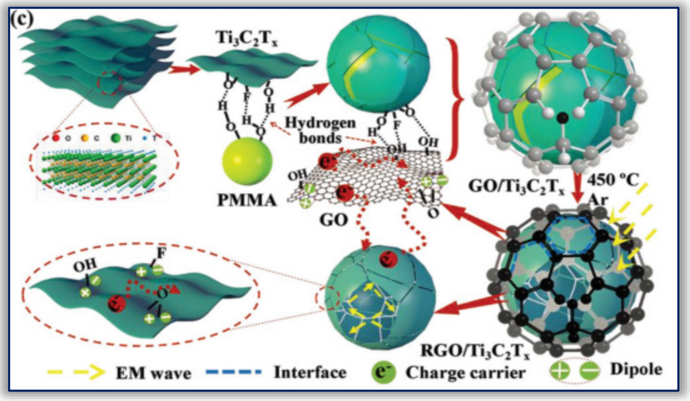

Figure 2 – Schematic demonstrating the EM absorption models (permission granted by the publisher) [74].

The majority of polymeric matrices are microwave–transparent in general, and the EM wave absorption in such materials is highly influenced by the strong integration between dielectric and magnetic losses of the fillers particulates [72]. An example of nanocomposite behavior in a microwave field is presented in Figure 2. Asymmetric charge distribution in a molecular structure or a mesoscopic dielectric interface can cause dielectric polarization. The dielectric characteristics of such a heterogeneous interface are caused by interfacial polarization in the microwave frequency range. Moreover, Joule heating loss is projected as a result of the existence of conductive characteristics in one of the contributing fillers [73].

The multiple–reflection is a third shielding mechanism that represents the internal reflections in the EM shield (see Figure 3). The contribution of multiple–reflection to the SE_T can be ignored if the distance among the reflecting surfaces or interfaces is greater than the penetration (skin) depth [25], or the absorption loss (SE_A) is less than −10 dB, i.e. only the reflection loss (SE_R) and the absorption loss contribute to the total SE value as mentioned in below Eq. 3 [27]:

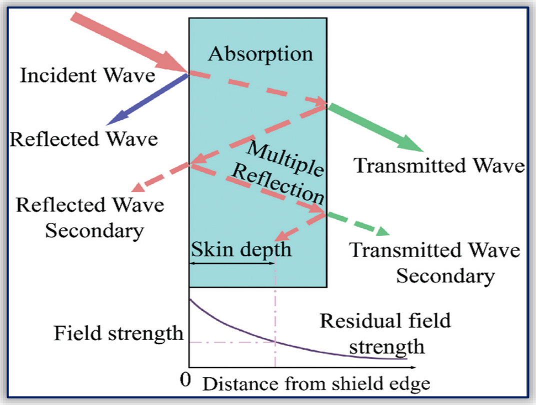

Figure 3 – Schematic demonstrating the shielding mechanisms[75] (permission granted by the publisher)

$$SE_T \approx SE_R + SE_A, \quad (3)$$

Compared to homogeneously conductive shielding material, the shielding mechanisms of polymer composites are more complex, since a large surface area is available for reflection and multiple–reflection. The first reflection of the EM wave from a conductive surface of the material must be differentiated from the multiple–reflection mechanism, the re–reflection of the waves already reflected [65].

3. EMI SHIELDING THROUGH MAGNETIC ABSORPTION OF THE MICROWAVE

— General overview

To improve device/equipment damage resistance and meet the growing demand for next–generation intelligent tech devices, highly efficient EMI shielding with low reflectivity remains a technical challenge to reduce the electromagnetic secondary pollution arising from the high reflection of EM wave irradiation which may limit their implementation in multiple domains such as electronics, communication, and other particular areas [76, 77].

Because of their wide range of practical uses, studies of absorption dominant shielding materials have gained popularity in recent years. Magnetic materials having dual magnetic/dielectric loss capability were thought to be an attractive candidate [78]. A reasonable microwave absorber (MA) design should take into account not only the intrinsic qualities of selected materials, but also optimize the architecture to obtain maximum EM wave absorption [79]. Accordingly, several designs and structures of microwave absorbers have been improved to promote effective absorption and reduce the reflection of EM waves [80].

Polymer–based nanocomposites such as metal/polymer composites, ferrite/polymer composites, and CNT/epoxy composites are commonly used as EM wave absorbers. To efficiently eliminate harmful EM waves a high–performance MA material with a broadband absorption capability is required in healthcare, electronic safety, and national defense security. Furthermore, in the sectors of aircraft, aviation, automobiles, and fast–growing new–generation microelectronics, MA materials with lightweight and small thickness will be highly valued [81].

High impedance fillers (i.e. low conductivity) are desirable to allow magnetic flux penetration and thus magnetic absorption. The interaction of an electromagnetic wave with a material is characterized by two key parameters, permittivity (ε) and permeability (μ). Under high–frequency conditions, these values can be complex in nature, with the real component (′ or μ') being a measure of how strongly an external electromagnetic wave interacts with the material and the imaginary component (ε" or μ") describing the dissipation of the wave as heat within the material [82].

The accompanying heat dissipation process is another feature of microwave–absorbing materials; when the input characteristic impedance of an absorber is matched to the characteristic impedance of free space, EM wave energy can be entirely absorbed and given off in the form of heat into a magnetic and dielectric material when a shielding material is subjected to EM radiation[83]. The Heat dissipation capability is a critical consideration for new–generation multifunctional EM absorbing materials, which can be solved by integrating high thermal conductivities of carbonaceous fillers in a polymer matrix with excellent MA capabilities [84]. When compared to other thermal conductive fillers CNTs, which have extremely high thermal conductivity (as high as 6000 W/m.K) for SWCNT and 3000 W/m.K for MWCNT at room temperature [85, 86]), offer significant advantages in the fabrication of thermal conductive nanocomposites. However, the thermal conductivities of polymer/CNT nanocomposites, on the other hand, are significantly lower when compared to the inherent thermal conductivity of CNTs [87]. This may be because many factors influence the thermal conductivity of such ncomposites, including the microstructure of the polymer matrix, and the dispersion status of CNTs, and the matrix–CNTs interfacial interaction [88]. It has been demonstrated that it can enhance stable CNT dispersion in matrices while also generating significant interfacial interaction with the polymer matrix [89].

To our knowledge, Based on the theory of EM wave absorption, the complementarity between magnetic and dielectric materials can highly tune the EM parameters like the attenuation constant and impedance matching, thereby improving the MA, according to the theory of EM wave absorption [90]. Furthermore, because pure single–phase carbon nano–fillers do not exhibit magnetic hysteresis loss, they have a limited role in EM wave absorption [91]. The formation of two–phase or three–phase heterostructures of carbon fillers and magnetic NPs is a practical solution for more efficiently absorbing EM waves and significantly reducing the impact of secondary EM radiation [92].

— Magnetic coating structure and/or layered structure based on multicomponent ferrites

So far, various research groups have reported a wide range of magnetic NPs such as Fe, Ni, Co ferrites and their multi–component ferrites like Fe_2O_3, Fe_3O_4, $CoFe_2O_4$ [93], CO_3O_4 [94], MnO_2, CrO_2, etc.) NPs [95] to optimize the impedance matching and absorption capability for various nanocomposites. In comparison to magnetic metals or alloys, ferromagnetic Ferro/ferric oxide (Fe_3O_4) NPs are shown to be an effective compound for fabricating MA materials relatively low cost, great antioxidant capacity, high Curie temperature, good thermal stability, and high chemical stability [5].

Magnetic hybrids are currently commonly employed as EM shielding materials. Magnetic materials having dual loss capability can, in reality, achieve balanced impedance match capability, which increases permeability values [78]. N. Li et al. claimed that the magnetic NPs coating structure (compact–coated or loose–coated) has a large influence on the total MA performance of coated CNTs, which is related to the coverage intensity of Fe_3O_4 NPs on the CNT surfaces. The high coverage density, according to the test findings, results in excellent complementary between the dielectric and the magnetic losses, multiple reflection and absorption of microwaves, and a high incidence probability [96]. According to P. F. Guan et al., interfacial polarization between Fe_3O_4 NPs and graphene take place in Fe_3O_4/graphene nanocomposite with self–assemble super–lattices of Fe_3O_4 NPs which exhibits both improved dielectric and magnetic losses at 2 – 18 GHz [97]. However, the Fe_3O_4 NPs, on the other hand, may obstruct the interconnections of individual graphene sheets in a polymer matrix, which would lower the electrical conductivity and thus the shielding performance of polymer composites [98]. Furthermore, a high nano–filler loading is always required to achieve a satisfactory SE, and large material thickness with reduced processability and productivity will result [84].

In the reference [99], an innovative design strategy for MA composite has been reported, in which the MA fillers (FeCo@rGO) are accumulated to form an initial microwave absorbing layer at the bottom of the waterborne polyurethane (WPU) film and the highly conductive fillers (Ag) are assembled as an ultra–thin layer on the top surface acts as microwave reflecting layer. The author indicated that the absorb–reflect–reabsorb mechanism would be induced by this layered structure. With a thickness of only 300 μm, this composite film has an excellent EMI SE of 50.5 dB and a low EMI reflection of 3.2 dB. In a similar manner, Y. Xu et al. fabricated flexible WPU composite films through assembling gradient shielding layers of Fe_3O_4 coated rGO and Ag–coated tetraneedle–like ZnO whisker (T–ZnO/Ag). When EM waves penetrate the composite film, this layered structure generates an "absorb–reflect–reabsorb" process. This composite film with a thickness of 0.5 mm showed outstanding EMI SE of 87.2 dB in the X band and reflection characteristics of 2.4 dB [15].

A sandwich–structured nanocomposite were created by Y. Zhang et al. using the following sequence: magnetic layers as the top and bottom layers (Fe_3O_4/PVA composite nanofibers) and a highly conductive layer as the intermediate layer ($Ti_3C_2T_x$/PVA composite nanofibers). The author claims that when EM waves strike the sandwich–structured surfaces, they interact with the Fe_3O_4 NPs, causing hysteresis loss. The EM wave is going through the magnetic layer, because of the substantial difference in

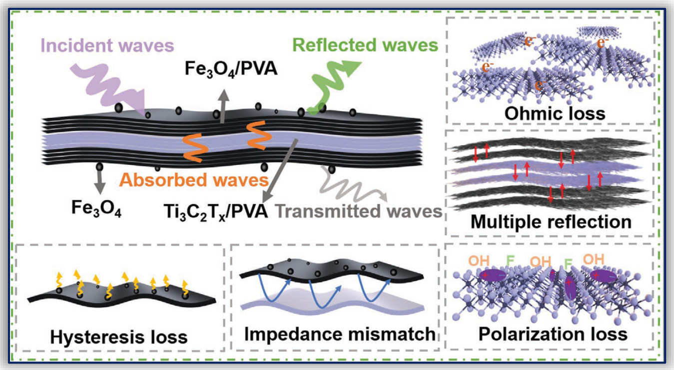

Figure 4 – Schematic illustrating of EMI shielding mechanism of sandwich–structured nanocomposite for EMI shielding (permission granted by the publisher) [100].

conductivity between the magnetic and conductive layer, there is a large impedance mismatch between the two. The remaining EM waves continue to pass through the $Ti_3C_2T_x$/PVA layer, and when they come into contact with the $Ti_3C_2T_x$ nanosheets, they will first experience polarization loss with $Ti_3C_2T_x$ surface functional groups like – OH, –F, etc (see Figure 4). Furthermore, when passing through the $Ti_3C_2T_x$ layer, charge carriers generate micro current, resulting in ohmic loss and a reduction in EM wave energy [100].

— Micro–wires based interconnected structure

Polymer–based nanocomposites in which ferromagnetic microwires with a size of (2–100 μm) are incorporated have attracted great interest in various industrial fields such as MA and EMI shielding owing to their large magneto–impedance and tunable magnetic characteristics 'flexible and sensitive tunability towards external magnetic field ' [101]. The magnetic characteristics of such microwires are highly dependent on the structure and behavior of the domain, which are frequency dependent, the reason for the variety of microwave properties of such wires and their composites [102]. In Ref [103], a modified Taylor–Ulitovskiy technique is used to produce glass–coated $Co_{60}Fe_{15}Si_{10}B_{15}$ microwires. To investigate the specific correlations between the microwave characteristics of the composites and aspect ratio and magnetic characteristics of the microwires, researchers employed as–cast microwires with various aspect ratios and treated microwires with joule annealing and glass removal. The author pretends that the internal stress modification via joule annealing offers significant impacts on formulating the MA intensity of such composites, by tuning the local anisotropy field and domain structure. Owing to their improved impedance match and intrinsic microwave attenuation characteristic, the composites with a shortcut microwires loading of 0.017 wt. % and a particularly large aspect ratio of 9 mm length, exhibit minimal reflection loss (RL) of 25.7 dB at 11.39 GHz with a broad absorption bandwidth.

Some time ago it was pointed out that the integration of carbon nanostructure, for example, could increase the electromagnetic and mechanical properties of microwires, since extreme absorption of the incident or reflected wave is highly desirable. However, such an approach often requires a precise tuning of the fillers parameters [104]. Y. Xu et al. synthesized a simple shielding system that uses magnetic microwires and graphene fibers, which are incorporated in a silicone resin in different arrangements since the lower electrical conductivity of graphene fibers reduces the reflection effectiveness of them compared to other graphene structures such as foam or film. The author explained that the microwires primarily contribute to the EM wave absorption characteristics owing to their electrical and magnetic properties while the graphene fibers contribute to the EM wave reflective characteristics owing to their electrical properties. It was able to enhance absorption efficiency and impedance matching by utilizing the synergistic effects of micro–wires and graphene fibers. The experimental results showed that the irregularly distributed layout made of short microwires/graphene fibers (equal amounts of graphene G and microwires M) exhibit a poor SE of 6 dB as compared to the regular layout with continuous fillers owing to the effect of low polarization and aspect ratio, as the interfacial polarization induced by the variations in permittivity and conductivity between the two regions governed to the total SE. The MMMGGG periodic layout achieved the maximum SE of 18 dB (98.4% attenuation) with only 0.059 wt %filler loading [105].

Another composite approach, which is similar in principle to the above idea, but uses shortcut CFs with Fe–based wires, was developed by Y. Luo et al. and shows a lower reflection coefficient (RC) in the frequency range, but its microwave behavior in the magnetic field was hard to tune. A comparison of another method claimed by the author is given when continuous CFs with microwires are incorporated into the composite 'to reduce RL, the microwires must be aligned perpendicular to the carbon fiber axis'. As a result, tunable permittivity and permeability were demonstrated, along with enhanced impedance matching. In fact, two issues exist due to the electrically reflective characteristic of CFs and therefore the difficulty in extracting relevant EM characteristics from their composites: (i) It is necessary to consider the orientation of CFs, which leads the metamaterial to be extremely anisotropic to incoming excitation directions [106].

— Graphene–based 3 D architecture

There is very extensive literature on the use of reduced graphene oxide (rGO) for the fabrication of EM wave absorbers. Owing to its excellent dielectric loss characteristics, multiple loss mechanism, and suitable impedance matching, rGO is the best option for MA compared to graphene and graphene oxide (GO) [107]. For instance, in the work of M. Zhang et al. a one–step, environmentally friendly, and inexpensive cation–assisted hydrothermal approach is used to produce lightweight rGO–3D aerogels, which are then uniformly distributed in a paraffin matrix. The uniform dispersion and loosely stacking of rGO gives a rich interfacial area for MA, which gives excellent MA performance with low filler loading (0.5 wt %) in a wide band frequency (8.0 ~ 18.0) GHz [108].
Four mechanisms are known to contribute to the polarization in the EM field; orientational (dipole–orientation), space charge (interfacial), ionic, and electronic polarization, which is responsible for the dielectric performance of the material. In a heterogeneous system formed with a polarized polymer matrix, interfacial and orientational

polarization are believed to be the predominant mechanisms. The ionic and electronic polarization only play a role at very high frequencies (over 1000 GHz). Therefore, their effects in the range of low microwave frequencies can be neglected [59]. Due to the fact that rGO sheets with reduced overlapping or coalescing GO nanosheets could provide a rich interfacial area for interfacial polarization, they are predicted to maximize the unique attributes of rGO to construct lightweight EMW absorbing materials [108]. In order to justify this claim, we recall the view of W. Xu et al. that the presence of rGO forms capacitor–like junctions that contribute to the accumulation of electrical charge at their interfacial areas, thus causing interface polarization. In addition, the remaining active groups and defects on the rGO surface, which were created by chemical reduction, induce polarization of the dipole orientation, which leads to an effective conversion of EM energy into thermal energy as well as excellent absorption performances [109].

As previously stated, the insertion of NPs of magnetic materials such as ferrites, magnetic oxides, hexaferrites, and others, in addition to carbonaceous fillers, strengthens the EMI shielding capabilities of polymer composites via microwave magnetic absorption [10, 110]. This opinion is reflected in the innovative design that has been demonstrated by H. Liu et al. in which lightweight nanocomposites were fabricated from polydimethylsiloxane matrix incorporating 3D graphene resulting from the integration of rGO foam and Ag–coated rGO aerogel film. In the sequence, the nanocomposites' structure is likened to; the Ag layer is on top, the rGO aerogel is in the middle, and the rGO foam layer is at the bottom. The rGO foam layer, according to the author, has a large number of bubble pores capable of absorbing EM waves via continual scattering and reflection, and also the surface roughness enables EM waves to penetrate the material nearly unhindered. The rGO aerogel film, on the other hand, has a porous structure and, when combined with the rGO foam layer, may absorb huge amounts of EM waves. When the EM wave passes across the Ag layer possess strong electrical conductivity, it can be reflected again for the secondary absorption, which greatly improves absorption loss and, accordingly, superior EMI–SE and a unique bi–directional differential performance provided. In addition, rGO foam also improves the internal reflection barriers [111]. Although these multilayered structures allow for more EMW propagation through absorbers, coating thicknesses must be raised proportionately [112]. Further work showed that with a 3D interconnected graphene network decorated with ZnO nanorods and cobalt ferrite NPs, a strong EMW absorption of around 93.7% power of the incident EM waves is achieved to confirm the fact that, porous 3D linked networks with their vast surface area, can support multiple reflections through diverse surfaces inside the network, hence improving EM wave absorption by trapping them within the network [113].

— MXene based 3D network

Several applications for the use of MXenes are currently being explored [114–116]. MXene, a 2D transition metal carbide and/or nitride, in particular, has also been introduced to replace existing metal–based shielding materials and is regarded as the most promising replacement due to its, strength, flexibility, and metal–equivalent ultrahigh conductivity [117], as well as numerous surface functional groups, hydrophilic surfaces, and unique 2D properties such as graphene and layered structure [118–120].

EMI shielding materials can be fabricated by using MXenes such as titanium carbide, Ti_3C_2Tx as a dielectric mediator due to their high conductivity and specific surface area, but they have some difficulties in assembling porous 3D structures [121]. This is due to the strong Van der Waals forces, and also the MXene flakes have a slight tendency to stack up to form a very dense structure. Inserting graphene nanosheets between MXen flakes appears to be an effective approach to preventing self–re–stacking of MXen flakes and to maintain high density [122]. Furthermore, the immaculate MXene films have poor processability, poor mechanical performance, and are costly [123]. MXene materials' insufficient mechanical characteristics limit their usability in some applications like as wearable electronic devices, weapons, and robot joints, which must be robust enough to withstand mechanical deformation [124].

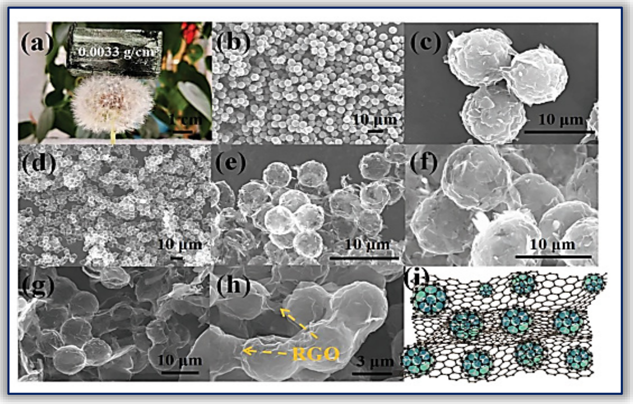

Figure 5 – Schematic illustrating of a) the picture of free–standing rGO/Ti3C2TX foam, SEM observation of b,c) $Ti_3C_2T_X$/PMMA spheres, d–f) hollow $Ti_3C_2T_X$ spheres, and g, h) RGO/$Ti_3C_2T_X$ foam, i) structural illustration of the rGO/$Ti_3C_2T_X$ foam (permission granted by the publisher) [74].

For the first time, a successful attempt was reported in which a sacrificial templating technique is used to combine Ti_3C_2TX and rGO spheres, hence the construction of the porous rGO–MXenes 3D foams with hollow core–shell architectures (Figure 5) through self–assembly that exhibit superior EM absorption performance in their composites [74]. To our knowledge, core/shell structured materials with more phase interfaces and a high specific surface area are set a new benchmark in the manufacture of EM wave absorbers. Such composites, for example, built on magnetic particles and carbon microspheres, could be regarded as a cost–effective technique for adjusting impedance match and improving EM wave attenuation [112]. Conceptually identical work utilizing a similar method was published by P. Song et al. a structural rGO honeycomb architecture (rGH) is formed using a template of the Al_2O_3 honeycomb architecture, using electrostatic adsorption MXene was self–assembled on the rGH to produce regular rGO–MXene with a honeycomb structure. The resulting rGO–MXene reinforced epoxy composite exhibits a superior EMI SE of 55 dB [125].

4. CONCLUSION

With the rapid evolution of digital electronics and communication devices, it is desirable to design lower–density materials to replace the conventional EMI shields such as normal metals. The recent article reviews numerous documented strategies for fabricating high–performance lightweight materials with superior EMI shielding efficiency. In particular, polymer–based nanocomposites with adequate magnetic/dielectric properties were reviewed. The outcome of various published articles supports the finding that the filler loading and the particle dispersion within the matrix as well as material thickness are considered key parameters for effective shielding. Several studies have been carried out to replace the conventional reflection–based shields with EM absorbers. Various structural composites integrating magnetic fillers and a hybrid of magnetic/dielectric fillers are being explored in this regard, and the most important findings of these materials are described in this review. According to the findings of numerous studies, micro–wires and complex architectures such as 3D foams and honeycombs in a polymer matrix have enabled a more functional design for EM absorption and EMI shielding.

Acknowledgments

This work is supported by research funding from the Innovation and Infrastructure program of the Islamic Development Bank IsDB. The author thanks IsDB for its financial support. The obvious opinions expressed in this paper are those of the authors, not those of the funders.

References

[1] Verma, P.; Bansala, T.; Chauhan, S. S.; Kumar, D.; Deveci, S.; Kumar, S., Electromagnetic interference shielding performance of carbon nanostructure reinforced, 3D printed polymer composites. Journal of Materials Science 2021, 56, 11769–11788.
[2] Gahlout, P.; Choudhary, V., EMI shielding response of polypyrrole–MWCNT/polyurethane composites. Synthetic Metals 2020, 266, 116414.
[3] Huang, L.; Li, J.; Wang, Z.; Li, Y.; He, X.; Yuan, Y., Microwave absorption enhancement of porous C@ CoFe2O4 nanocomposites derived from eggshell membrane. Carbon 2019, 143, 507–516.
[4] Lee, S. H.; Yu, S.; Shahzad, F.; Kim, W. N.; Park, C.; Hong, S. M.; Koo, C. M., Density–tunable lightweight polymer composites with dual–functional ability of efficient EMI shielding and heat dissipation. Nanoscale 2017, 9, 13432–13440.
[5] Li, Z.; Li, X.; Zong, Y.; Tan, G.; Sun, Y.; Lan, Y.; He, M.; Ren, Z.; Zheng, X., Solvothermal synthesis of nitrogen–doped graphene decorated by superparamagnetic Fe3O4 nanoparticles and their applications as enhanced synergistic microwave absorbers. Carbon 2017, 115, 493–502.
[6] Lin, J. C., Human exposure to RF, microwave, and millimeter–wave electromagnetic radiation [Health Effects]. IEEE Microwave Magazine 2016, 17, 32–36.
[7] Kumaran, R.; Alagar, M.; Dinesh Kumar, S.; Subramanian, V.; Dinakaran, K., Ag induced electromagnetic interference shielding of Ag–graphite/PVDF flexible nanocomposites thinfilms. Applied Physics Letters 2015, 107, 113107.
[8] Pande, A.; Gairola, P.; Sambyal, P.; Gairola, S.; Kumar, V.; Singh, K.; Dhawan, S., Electromagnetic shielding behavior of polyaniline using Red Mud (industrial waste) as filler in the X–band (8.2–12.4 GHz) frequency range. Materials Chemistry and Physics 2017, 189, 22–27.
[9] Shin, B.; Mondal, S.; Lee, M.; Kim, S.; Huh, Y.–I.; Nah, C., Flexible thermoplastic polyurethane–carbon nanotube composites for electromagnetic interference shielding and thermal management. Chemical Engineering Journal 2021, 418, 129282.
[10] Choudhary, H. K.; Kumar, R.; Pawar, S. P.; Sahoo, B., Role of graphitization–controlled conductivity in enhancing absorption dominated EMI shielding behavior of pyrolysis–derived Fe3C@ C–PVDF nanocomposites. Materials Chemistry and Physics 2021, 263, 124429.
[11] Dravid, S. V.; Bhosale, S. D.; Datar, S.; Goyal, R., Nickel Nanoparticle–Filled High–Performance Polymeric Nanocomposites for EMI Shielding Applications. Journal of Electronic Materials 2020, 49, 1630–1637.
[12] Li, J.; Zhao, X.; Wu, W.; Ji, X.; Lu, Y.; Zhang, L., Bubble–templated rGO–graphene nanoplatelet foams encapsulated in silicon rubber for electromagnetic interference shielding and high thermal conductivity. Chemical Engineering Journal 2021, 415, 129054.
[13] Ren, W.; Yang, Y.; Yang, J.; Duan, H.; Zhao, G.; Liu, Y., Multifunctional and corrosion resistant poly (phenylene sulfide)/Ag composites for electromagnetic interference shielding. Chemical Engineering Journal 2021, 415, 129052.
[14] Shayesteh Zeraati, A.; Mende Anjaneyalu, A.; Pawar, S. P.; Abouelmagd, A.; Sundararaj, U., Effect of secondary filler properties and geometry on the electrical, dielectric, and electromagnetic interference shielding properties of carbon nanotubes/polyvinylidene fluoride nanocomposites. Polymer Engineering & Science 2021, 61, 959–970.
[15] Xu, Y.; Yang, Y.; Yan, D.–X.; Duan, H.; Zhao, G.; Liu, Y., Gradient structure design of flexible waterborne polyurethane conductive films for ultraefficient electromagnetic shielding with low reflection characteristic. ACS applied materials & interfaces 2018, 10, 19143–19152.
[16] Kim, H.; Kim, K.; Lee, C.; Joo, J.; Cho, S.; Yoon, H.; Pejaković, D.; Yoo, J.–W.; Epstein, A., Electrical conductivity and electromagnetic interference shielding of multiwalled carbon nanotube composites containing Fe catalyst. Applied physics letters 2004, 84, 589–591.
[17] Guo, H.; Li, Y.; Ji, Y.; Chen, Y.; Liu, K.; Shen, B.; He, S.; Duan, G.; Han, J.; Jiang, S., Highly flexible carbon nanotubes/aramid nanofibers composite papers with ordered and layered structures for efficient electromagnetic interference shielding. Composites Communications 2021, 27, 100879.

[18] Wang, M.; Tang, X.–H.; Cai, J.–H.; Wu, H.; Shen, J.–B.; Guo, S.–Y., Construction, mechanism and prospective of conductive polymer composites with multiple interfaces for electromagnetic interference shielding: A review. Carbon 2021, 177, 377–402.
[19] Li, X.; Zeng, S.; E, S.; Liang, L.; Bai, Z.; Zhou, Y.; Zhao, B.; Zhang, R., Quick heat dissipation in absorption–dominated microwave shielding properties of flexible poly (vinylidene fluoride)/carbon nanotube/Co composite films with anisotropy–shaped Co (flowers or chains). ACS applied materials & interfaces 2018, 10, 40789–40799.
[20] Han, G.; Ma, Z.; Zhou, B.; He, C.; Wang, B.; Feng, Y.; Ma, J.; Sun, L.; Liu, C., Cellulose–based Ni–decorated graphene magnetic film for electromagnetic interference shielding. Journal of Colloid and Interface Science 2021, 583, 571–578.
[21] Park, J.–B.; Rho, H.; Cha, A.–N.; Bae, H.; Lee, S. H.; Ryu, S.–W.; Jeong, T.; Ha, J.–S., Transparent carbon nanotube web structures with Ni–Pd nanoparticles for electromagnetic interference (EMI) shielding of advanced display devices. Applied Surface Science 2020, 516, 145745.
[22] Zeranska-Chudek, K.; Lapinska, A.; Siemion, A.; Jastrzębska, A. M.; Zdrojek, M., Terahertz time domain spectroscopy of graphene and MXene polymer composites. Journal of Applied Polymer Science 2021, 138, 49962.
[23] Das, S.; Sharma, S.; Yokozeki, T.; Dhakate, S., Conductive layer–based multifunctional structural composites for electromagnetic interference shielding. Composite Structures 2021, 261, 113293.
[24] Quan, B.; Liang, X.; Ji, G.; Lv, J.; Dai, S.; Xu, G.; Du, Y., Laminated graphene oxide–supported high–efficiency microwave absorber fabricated by an in situ growth approach. Carbon 2018, 129, 310–320.
[25] Chung, D., Electromagnetic interference shielding effectiveness of carbon materials. carbon 2001, 39, 279–285.
[26] Nath, K.; Ghosh, S.; Ghosh, S. K.; Das, P.; Das, N. C., Facile preparation of light-weight biodegradable and electrically conductive polymer based nanocomposites for superior electromagnetic interference shielding effectiveness. Journal of Applied Polymer Science 2021, 138, 50514.
[27] Singh, A. K.; Shishkin, A.; Koppel, T.; Gupta, N., A review of porous lightweight composite materials for electromagnetic interference shielding. Composites Part B: Engineering 2018, 149, 188–197.
[28] Yu, W.–C.; Xu, J.–Z.; Wang, Z.–G.; Huang, Y.–F.; Yin, H.–M.; Xu, L.; Chen, Y.–W.; Yan, D.–X.; Li, Z.–M., Constructing highly oriented segregated structure towards high–strength carbon nanotube/ultrahigh–molecular–weight polyethylene composites for electromagnetic interference shielding. Composites Part A: Applied Science and Manufacturing 2018, 110, 237–245.
[29] Li, J.; Peng, W.–J.; Fu, Z.–J.; Tang, X.–H.; Wu, H.; Guo, S.; Wang, M., Achieving high electrical conductivity and excellent electromagnetic interference shielding in poly (lactic acid)/silver nanocomposites by constructing large–area silver nanoplates in polymer matrix. Composites Part B: Engineering 2019, 171, 204–213.
[30] Yu, W.–C.; Wang, T.; Liu, Y.–H.; Wang, Z.–G.; Xu, L.; Tang, J.–H.; Dai, K.; Duan, H.–J.; Xu, J.–Z.; Li, Z.–M., Superior and highly absorbed electromagnetic interference shielding performance achieved by designing the reflection–absorption–integrated shielding compartment with conductive wall and lossy core. Chemical Engineering Journal 2020, 393, 124644.
[31] Cui, J.; Zhou, S., Facile fabrication of highly conductive polystyrene/nanocarbon composites with robust interconnected network via electrostatic attraction strategy. Journal of Materials Chemistry C 2018, 6, 550–557.
[32] Vovchenko, L.; Matzui, L.; Oliynyk, V.; Milovanov, Y.; Mamunya, Y.; Volynets, N.; Plyushch, A.; Kuzhir, P., Polyethylene composites with segregated carbon nanotubes network: low frequency plasmons and high electromagnetic interference shielding efficiency. Materials 2020, 13, 1118.
[33] Lecocq, H.; Garois, N.; Lhost, O.; Girard, P.–F.; Cassagnau, P.; Serghei, A., Polypropylene/carbon nanotubes composite materials with enhanced electromagnetic interference shielding performance: Properties and modeling. Composites Part B: Engineering 2020, 189, 107866.
[34] Zhang, Y.–P.; Zhou, C.–G.; Sun, W.–J.; Wang, T.; Jia, L.–C.; Yan, D.–X.; Li, Z.–M., Injection molding of segregated carbon nanotube/polypropylene composite with enhanced electromagnetic interference shielding and mechanical performance. Composites Science and Technology 2020, 197, 108253.
[35] Kim, J.; Kim, G.; Kim, S.–Y.; Lee, S.; Kim, Y.; Lee, J.; Kim, J.; Jung, Y. C.; Kwon, J.; Han, H., Fabrication of highly flexible electromagnetic interference shielding polyimide carbon black composite using hot–pressing method. Composites Part B: Engineering 2021, 221, 109010.
[36] Gu, J.; Hu, S.; Ji, H.; Feng, H.; Zhao, W.; Wei, J.; Li, M., Multi–layer silver nanowire/polyethylene terephthalate mesh structure for highly efficient transparent electromagnetic interference shielding. Nanotechnology 2020, 31, 185303.
[37] Nimbalkar, P.; Korde, A.; Goyal, R., Electromagnetic interference shielding of polycarbonate/GNP nanocomposites in X–band. Materials Chemistry and Physics 2018, 206, 251–258.
[38] Tolvanen, J.; Hannu, J.; Hietala, M.; Kordas, K.; Jantunen, H., Biodegradable multiphase poly (lactic acid)/biochar/graphite composites for electromagnetic interference shielding. Composites Science and Technology 2019, 181, 107704.
[39] Tang, X.–H.; Li, J.; Tan, Y.–J.; Cai, J.–H.; Liu, J.–H.; Wang, M., Achieve high performance microwave shielding in poly (ε–caprolactone)/multi–wall carbon nanotube composites via balancing absorption in conductive domains and multiple scattering at interfaces. Applied Surface Science 2020, 508, 145178.
[40] Wang, Y.–Y.; Zhou, Z.–H.; Zhou, C.–G.; Sun, W.–J.; Gao, J.–F.; Dai, K.; Yan, D.–X.; Li, Z.–M., Lightweight and robust carbon nanotube/polyimide foam for efficient and heat–resistant electromagnetic interference shielding and microwave absorption. ACS Applied Materials & Interfaces 2020, 12, 8704–8712.
[41] Tunakova, V.; Tunak, M., Carbon–fiber reinforcements for epoxy composites with electromagnetic radiation protection—prediction of electromagnetic shielding ability. Composites Science and Technology 2021, 215, 109029.
[42] Ju, J.; Kuang, T.; Ke, X.; Zeng, M.; Chen, Z.; Zhang, S.; Peng, X., Lightweight multifunctional polypropylene/carbon nanotubes/carbon black nanocomposite foams with segregated structure, ultralow percolation threshold and enhanced electromagnetic interference shielding performance. Composites Science and Technology 2020, 193, 108116.
[43] Duan, H.; Zhu, H.; Yang, J.; Gao, J.; Yang, Y.; Xu, L.; Zhao, G.; Liu, Y., Effect of carbon nanofiller dimension on synergistic EMI shielding network of epoxy/metal conductive foams. Composites Part A: Applied Science and Manufacturing 2019, 118, 41–48.
[44] Mondal, S.; Ravindren, R.; Bhawal, P.; Shin, B.; Ganguly, S.; Nah, C.; Das, N. C., Combination effect of carbon nanofiber and ketjen carbon black hybrid nanofillers on mechanical, electrical, and electromagnetic interference shielding properties of chlorinated polyethylene nanocomposites. Composites Part B: Engineering 2020, 197, 108071.
[45] Kargar, F.; Barani, Z.; Balinskiy, M.; Magana, A. S.; Lewis, J. S.; Balandin, A. A., Dual-functional graphene composites for electromagnetic shielding and thermal management. Advanced Electronic Materials 2019, 5, 1800558.
[46] Feng, L.; Zuo, Y.; He, X.; Hou, X.; Fu, Q.; Li, H.; Song, Q., Development of light cellular carbon nanotube@graphene/carbon nanocomposites with effective mechanical and EMI shielding performance. Carbon 2020, 168, 719–731.

[47] Zhao, H.; Xu, X.; Fan, D.; Xu, P.; Wang, F.; Cui, L.; Han, X.; Du, Y., Anchoring porous carbon nanoparticles on carbon nanotubes as a high–performance composite with a unique core–sheath structure for electromagnetic pollution precaution. Journal of Materials Chemistry A 2021, 9, 22489–22500.
[48] Yuan, D.; Guo, H.; Ke, K.; Manas–Zloczower, I., Recyclable conductive epoxy composites with segregated filler network structure for EMI shielding and strain sensing. Composites Part A: Applied Science and Manufacturing 2020, 132, 105837.
[49] Zhao, S.; Yan, Y.; Gao, A.; Zhao, S.; Cui, J.; Zhang, G., Flexible Polydimethylsilane Nanocomposites Enhanced with a Three–Dimensional Graphene/Carbon Nanotube Bicontinuous Framework for High–Performance Electromagnetic Interference Shielding. ACS Applied Materials & Interfaces 2018, 10, 26723–26732.
[50] Quan, B.; Xu, G.; Gu, W.; Sheng, J.; Ji, G., Cobalt nanoparticles embedded nitrogen–doped porous graphitized carbon composites with enhanced microwave absorption performance. Journal of Colloid and Interface Science 2019, 533, 297–303.
[51] Pavlou, C.; Pastore Carbone, M. G.; Manikas, A. C.; Trakakis, G.; Koral, C.; Papari, G.; Andreone, A.; Galiotis, C., Effective EMI shielding behaviour of thin graphene/PMMA nanolaminates in the THz range. Nature Communications 2021, 12, 1–9.
[52] Liang, C.; Song, P.; Qiu, H.; Zhang, Y.; Ma, X.; Qi, F.; Gu, H.; Kong, J.; Cao, D.; Gu, J., Constructing interconnected spherical hollow conductive networks in silver platelets/reduced graphene oxide foam/epoxy nanocomposites for superior electromagnetic interference shielding effectiveness. Nanoscale 2019, 11, 22590–22598.
[53] Choudhary, H. K.; Kumar, R.; Pawar, S. P.; Sundararaj, U.; Sahoo, B., Superiority of graphite coated metallic–nanoparticles over graphite coated insulating–nanoparticles for enhancing EMI shielding. New Journal of Chemistry 2021, 45, 4592–4600.
[54] Jang, J. O.; Park, J. W., In; Google Patents: 2002.
[55] IEEE Standard for Safety Levels with Respect to Human Exposure to Radio Frequency Electromagnetic Fields, 3 kHz to 300 GHz. IEEE Std C95.1–2005 (Revision of IEEE Std C95.1–1991) 2006, 1–238.
[56] Protection, I. C. o. N.–I. R., ICNIRP statement on the "Guidelines for limiting exposure to time–varying electric, magnetic, and electromagnetic fields (up to 300 GHz)". Health physics 2009, 97, 257–258.
[57] Geetha, S.; Satheesh Kumar, K.; Rao, C. R.; Vijayan, M.; Trivedi, D., EMI shielding: Methods and materials—A review. Journal of applied polymer science 2009, 112, 2073–2086.
[58] Wang, Y.; Jing, X., Intrinsically conducting polymers for electromagnetic interference shielding. Polymers for advanced technologies 2005, 16, 344–351.
[59] Kruželák, J.; Kvasničáková, A.; Hložeková, K.; Hudec, I., Progress in polymers and polymer composites used as efficient materials for EMI shielding. Nanoscale Advances 2021, 3, 123–172.
[60] Gaoui, B.; Hadjadj, A.; Kious, M., Enhancement of the shielding effectiveness of multilayer materials by gradient thickness in the stacked layers. Journal of Materials Science: Materials in Electronics 2017, 28, 11292–11299.
[61] Weng, C.; Xing, T.; Jin, H.; Wang, G.; Dai, Z.; Pei, Y.; Liu, L.; Zhang, Z., Mechanically robust ANF/MXene composite films with tunable electromagnetic interference shielding performance. Composites Part A: Applied Science and Manufacturing 2020, 135, 105927.
[62] Joshi, A.; Datar, S., Carbon nanostructure composite for electromagnetic interference shielding. Pramana 2015, 84, 1099–1116.
[63] Liang, C.; Qiu, H.; Han, Y.; Gu, H.; Song, P.; Wang, L.; Kong, J.; Cao, D.; Gu, J., Superior electromagnetic interference shielding 3D graphene nanoplatelets/reduced graphene oxide foam/epoxy nanocomposites with high thermal conductivity. Journal of Materials Chemistry C 2019, 7, 2725–2733.
[64] Kashi, S.; Gupta, R. K.; Bhattacharya, S. N.; Varley, R. J., Experimental and simulation study of effect of thickness on performance of (butylene adipate–co–terephthalate) and poly lactide nanocomposites incorporated with graphene as stand–alone electromagnetic interference shielding and metal–backed microwave absorbers. Composites Science and Technology 2020, 195, 108186.
[65] Al–Saleh, M. H.; Sundararaj, U., Electromagnetic interference shielding mechanisms of CNT/polymer composites. Carbon 2009, 47, 1738–1746.
[66] Oh, K.; Hong, S. M.; Seo, Y., Effect of crosslinking reaction on the electromagnetic interference shielding of a Fe–Si–Al alloy (Sendust)/polymer composite at high frequency. Polymers for advanced technologies 2014, 25, 1366–1370.
[67] Yu, W.–C.; Zhang, G.–Q.; Liu, Y.–H.; Xu, L.; Yan, D.–X.; Huang, H.–D.; Tang, J.–H.; Xu, J.–Z.; Li, Z.–M., Selective electromagnetic interference shielding performance and superior mechanical strength of conductive polymer composites with oriented segregated conductive networks. Chemical Engineering Journal 2019, 373, 556–564.
[68] Zhang, B.; Feng, Y.; Xiong, J.; Yang, Y.; Lu, H., Microwave–absorbing properties of de–aggregated flake–shaped carbonyl–iron particle composites at 2–18 GHz. IEEE Transactions on Magnetics 2006, 42, 1778–1781.
[69] Duan, W.; Yin, X.; Li, Q.; Schlier, L.; Greil, P.; Travitzky, N., A review of absorption properties in silicon–based polymer derived ceramics. Journal of the European Ceramic Society 2016, 36, 3681–3689.
[70] Biswas, S.; Arief, I.; Panja, S. S.; Bose, S., Absorption–dominated electromagnetic wave suppressor derived from ferrite–doped cross–linked graphene framework and conducting carbon. ACS applied materials & interfaces 2017, 9, 3030–3039.
[71] Quan, L.; Qin, F.; Li, Y.; Estevez, D.; Fu, G.; Wang, H.; Peng, H., Magnetic graphene enabled tunable microwave absorber via thermal control. Nanotechnology 2018, 29, 245706.
[72] Abbas, S.; Chandra, M.; Verma, A.; Chatterjee, R.; Goel, T., Complex permittivity and microwave absorption properties of a composite dielectric absorber. Composites Part A: applied science and manufacturing 2006, 37, 2148–2154.
[73] Sun, D.; Zou, Q.; Qian, G.; Sun, C.; Jiang, W.; Li, F., Controlled synthesis of porous Fe3O4–decorated graphene with extraordinary electromagnetic wave absorption properties. Acta materialia 2013, 61, 5829–5834.
[74] Li, X.; Yin, X.; Song, C.; Han, M.; Xu, H.; Duan, W.; Cheng, L.; Zhang, L., Self-Assembly Core–Shell Graphene-Bridged Hollow MXenes Spheres 3D Foam with Ultrahigh Specific EM Absorption Performance. Advanced Functional Materials 2018, 28, 1803938.
[75] Chen, R.; Yu, R.; Pei, X.; Wang, W.; Li, D.; Xu, Z.; Luo, S.; Tang, Y.; Deng, H., Interface design of carbon filler/polymer composites for electromagnetic interference shielding. New Journal of Chemistry 2021, 45, 8370–8385.
[76] Prasad, J.; Singh, A. K.; Yadav, A. N.; Kumar, A.; Tomar, M.; Srivastava, A.; Kumar, P.; Gupta, V.; Singh, K., Molybdenum disulfide–wrapped carbon nanotube–reduced graphene oxide (CNT/MoS2–rGO) nanohybrids for excellent and fast removal of electromagnetic interference pollution. ACS Applied Materials & Interfaces 2020, 12, 40828–40837.
[77] Yang, J.; Liao, X.; Li, J.; He, G.; Zhang, Y.; Tang, W.; Wang, G.; Li, G., Light–weight and flexible silicone rubber/MWCNTs/Fe3O4 nanocomposite foams for efficient electromagnetic interference shielding and microwave absorption. Composites Science and Technology 2019, 181, 107670.

[78] Jia, Z.; Wang, C.; Feng, A.; Shi, P.; Zhang, C.; Liu, X.; Wang, K.; Wu, G., A low–dielectric decoration strategy to achieve absorption dominated electromagnetic shielding material. Composites Part B: Engineering 2020, 183, 107690.
[79] Quan, B.; Liang, X.; Yi, H.; Gong, H.; Ji, G.; Chen, J.; Xu, G.; Du, Y., Constructing hierarchical porous nanospheres for versatile microwave response approaches: the effect of architectural design. Dalton Transactions 2017, 46, 14264–14269.
[80] Li, Y.; Yang, H.; Hao, X.; Sun, N.; Du, J.; Cao, M., Enhanced electromagnetic interference shielding with low reflection induced by heterogeneous double–layer structure in BiFeO3/BaFe7 (MnTi) 2.5 O19 composite. Journal of Alloys and Compounds 2019, 772, 99–104.
[81] Zhang, Y.; Huang, Y.; Zhang, T.; Chang, H.; Xiao, P.; Chen, H.; Huang, Z.; Chen, Y., Broadband and tunable high-performance microwave absorption of an ultralight and highly compressible graphene foam. Advanced materials 2015, 27, 2049–2053.
[82] Charles, A. D.; Rider, A. N.; Brown, S. A.; Wang, C. H., Multifunctional magneto–polymer matrix composites for electromagnetic interference suppression, sensors and actuators. Progress in Materials Science 2021, 115, 100705.
[83] Dar, M. A.; Kotnala, R.; Verma, V.; Shah, J.; Siddiqui, W.; Alam, M., High magneto–crystalline anisotropic core–shell structured Mn0. 5Zn0. 5Fe2O4/polyaniline nanocomposites prepared by in situ emulsion polymerization. The Journal of Physical Chemistry C 2012, 116, 5277–5287.
[84] Arief, I.; Biswas, S.; Bose, S., FeCo–anchored reduced graphene oxide framework–based soft composites containing carbon nanotubes as highly efficient microwave absorbers with excellent heat dissipation ability. ACS applied materials & interfaces 2017, 9, 19202–19214.
[85] Huang, H.; Liu, C.; Wu, Y.; Fan, S., Aligned carbon nanotube composite films for thermal management. Advanced materials 2005, 17, 1652–1656.
[86] Biercuk, M.; Llaguno, M. C.; Radosavljevic, M.; Hyun, J.; Johnson, A. T.; Fischer, J. E., Carbon nanotube composites for thermal management. Applied physics letters 2002, 80, 2767–2769.
[87] Han, Z.; Fina, A., Thermal conductivity of carbon nanotubes and their polymer nanocomposites: A review. Progress in polymer science 2011, 36, 914–944.
[88] Zhang, W.–b.; Zhang, Z.–x.; Yang, J.–h.; Huang, T.; Zhang, N.; Zheng, X.–t.; Wang, Y.; Zhou, Z.–w., Largely enhanced thermal conductivity of poly (vinylidene fluoride)/carbon nanotube composites achieved by adding graphene oxide. Carbon 2015, 90, 242–254.
[89] Zhang, C.; Huang, S.; Tjiu, W. W.; Fan, W.; Liu, T., Facile preparation of water–dispersible graphene sheets stabilized by acid–treated multi–walled carbon nanotubes and their poly (vinyl alcohol) composites. Journal of Materials Chemistry 2012, 22, 2427–2434.
[90] Wang, Y.; Gao, X.; Fu, Y.; Wu, X.; Wang, Q.; Zhang, W.; Luo, C., Enhanced microwave absorption performances of polyaniline/graphene aerogel by covalent bonding. Composites Part B: Engineering 2019, 169, 221–228.
[91] Lee, S.–H.; Kang, D.; Oh, I.–K., Multilayered graphene–carbon nanotube–iron oxide three–dimensional heterostructure for flexible electromagnetic interference shielding film. Carbon 2017, 111, 248–257.
[92] Liu, Y.; Song, D.; Wu, C.; Leng, J., EMI shielding performance of nanocomposites with MWCNTs, nanosized Fe3O4 and Fe. Composites Part B: Engineering 2014, 63, 34–40.
[93] Lim, G.–H.; Woo, S.; Lee, H.; Moon, K.–S.; Sohn, H.; Lee, S.–E.; Lim, B., Mechanically robust magnetic carbon nanotube papers prepared with CoFe2O4 nanoparticles for electromagnetic interference shielding and magnetomechanical actuation. ACS applied materials & interfaces 2017, 9, 40628–40637.
[94] Chen, Y.; Zhang, H.–B.; Huang, Y.; Jiang, Y.; Zheng, W.–G.; Yu, Z.–Z., Magnetic and electrically conductive epoxy/graphene/carbonyl iron nanocomposites for efficient electromagnetic interference shielding. Composites Science and Technology 2015, 118, 178–185.
[95] Chaudhary, A.; Kumar, R.; Teotia, S.; Dhawan, S.; Dhakate, S. R.; Kumari, S., Integration of MCMBs/MWCNTs with Fe 3 O 4 in a flexible and light weight composite paper for promising EMI shielding applications. Journal of Materials Chemistry C 2017, 5, 322–332.
[96] Li, N.; Huang, G.–W.; Li, Y.–Q.; Xiao, H.–M.; Feng, Q.–P.; Hu, N.; Fu, S.–Y., Enhanced microwave absorption performance of coated carbon nanotubes by optimizing the Fe3O4 nanocoating structure. ACS applied materials & interfaces 2017, 9, 2973–2983.
[97] Guan, P.; Zhang, X.; Guo, J., Assembled Fe3O4 nanoparticles on graphene for enhanced electromagnetic wave losses. Applied Physics Letters 2012, 101, 153108.
[98] Chen, Y.; Wang, Y.; Zhang, H.–B.; Li, X.; Gui, C.–X.; Yu, Z.–Z., Enhanced electromagnetic interference shielding efficiency of polystyrene/graphene composites with magnetic Fe3O4 nanoparticles. Carbon 2015, 82, 67–76.
[99] Zhu, H.; Yang, Y.; Sheng, A.; Duan, H.; Zhao, G.; Liu, Y., Layered structural design of flexible waterborne polyurethane conductive film for excellent electromagnetic interference shielding and low microwave reflectivity. Applied Surface Science 2019, 469, 1–9.
[100] Zhang, Y.; Ruan, K.; Gu, J., Flexible sandwich-structured electromagnetic interference shielding nanocomposite films with excellent thermal conductivities. Small 2021, 17, 2101951.
[101] Uddin, A.; Qin, F.; Estevez, D.; Jiang, S.; Panina, L.; Peng, H., Microwave programmable response of Co–based microwire polymer composites through wire microstructure and arrangement optimization. Composites Part B: Engineering 2019, 176, 107190.
[102] Zhao, Y.; Zheng, X.; Qin, F.; Estevez, D.; Luo, Y.; Wang, H.; Peng, H., A self–sensing microwire/epoxy composite optimized by dual interfaces and periodical structural integrity. Composites Part B: Engineering 2020, 182, 107606.
[103] Zheng, X.; Qin, F.; Wang, H.; Mai, Y.–W.; Peng, H., Microwave absorbing properties of composites containing ultra–low loading of optimized microwires. Composites Science and Technology 2017, 151, 62–70.
[104] Estevez, D.; Qin, F.; Luo, Y.; Quan, L.; Mai, Y.–W.; Panina, L.; Peng, H.–X., Tunable negative permittivity in nano–carbon coated magnetic microwire polymer metacomposites. Composites Science and Technology 2019, 171, 206–217.
[105] Xu, Y.; Uddin, A.; Estevez, D.; Luo, Y.; Peng, H.; Qin, F., Lightweight microwire/graphene/silicone rubber composites for efficient electromagnetic interference shielding and low microwave reflectivity. Composites Science and Technology 2020, 189, 108022.
[106] Luo, Y.; Estevez, D.; Scarpa, F.; Panina, L.; Wang, H.; Qin, F.; Peng, H.–X., Microwave properties of metacomposites containing carbon fibres and ferromagnetic microwires. Research 2019, 2019.
[107] Quan, L.; Qin, F.; Estevez, D.; Wang, H.; Peng, H., Magnetic graphene for microwave absorbing application: towards the lightest graphene–based absorber. Carbon 2017, 125, 630–639.
[108] Zhang, M.; Fang, X.; Zhang, Y.; Guo, J.; Gong, C.; Estevez, D.; Qin, F.; Zhang, J., Ultralight reduced graphene oxide aerogels prepared by cation–assisted strategy for excellent electromagnetic wave absorption. Nanotechnology 2020, 31, 275707.
[109] Xu, W.; Wang, G.–S.; Yin, P.–G., Designed fabrication of reduced graphene oxides/Ni hybrids for effective electromagnetic absorption and shielding. Carbon 2018, 139, 759–767.
[110] Huangfu, Y.; Liang, C.; Han, Y.; Qiu, H.; Song, P.; Wang, L.; Kong, J.; Gu, J., Fabrication and investigation on the Fe3O4/thermally annealed graphene aerogel/epoxy electromagnetic interference shielding nanocomposites. Composites Science and Technology 2019, 169, 70–75.

[111] Liu, H.; Xu, Y.; Cao, J.–P.; Han, D.; Yang, Q.; Li, R.; Zhao, F., Skin structured silver/three–dimensional graphene/polydimethylsiloxane composites with exceptional electromagnetic interference shielding effectiveness. Composites Part A: Applied Science and Manufacturing 2021, 148, 106476.
[112] Han, M.; Yin, X.; Ren, S.; Duan, W.; Zhang, L.; Cheng, L., Core/shell structured C/ZnO nanoparticles composites for effective electromagnetic wave absorption. RSC advances 2016, 6, 6467–6474.
[113] Gupta, S.; Sharma, S. K.; Pradhan, D.; Tai, N.–H., Ultra–light 3D reduced graphene oxide aerogels decorated with cobalt ferrite and zinc oxide perform excellent electromagnetic interference shielding effectiveness. Composites Part A: Applied Science and Manufacturing 2019, 123, 232–241.
[114] Rajavel, K.; Yu, X.; Zhu, P.; Hu, Y.; Sun, R.; Wong, C., Exfoliation and Defect Control of Two–Dimensional Few–Layer MXene $Ti_3C_2T_x$ for Electromagnetic Interference Shielding Coatings. ACS Applied Materials & Interfaces 2020, 12, 49737–49747.
[115] Liu, G.; Xiong, Q.; Xu, Y.; Fang, Q.; Leung, K. C.–F.; Sang, M.; Xuan, S.; Hao, L., Magnetically separable MXene@Fe_3O_4/Au/PDA nanosheets with photothermal–magnetolytic coupling antibacterial performance. Applied Surface Science 2022, 590, 153125.
[116] Yang, M.; Yang, Z.; Lv, C.; Wang, Z.; Lu, Z.; Lu, G.; Jia, X.; Wang, C., Electrospun bifunctional MXene–based electronic skins with high performance electromagnetic shielding and pressure sensing. Composites Science and Technology 2022, 221, 109313.
[117] Yun, T.; Kim, H.; Iqbal, A.; Cho, Y. S.; Lee, G. S.; Kim, M.–K.; Kim, S. J.; Kim, D.; Gogotsi, Y.; Kim, S. O.; Koo, C. M., Electromagnetic Shielding of Monolayer MXene Assemblies. Advanced Materials 2020, 32, 1906769.
[118] Li, Y.; Zhou, B.; Shen, Y.; He, C.; Wang, B.; Liu, C.; Feng, Y.; Shen, C., Scalable manufacturing of flexible, durable $Ti_3C_2T_x$ MXene/Polyvinylidene fluoride film for multifunctional electromagnetic interference shielding and electro/photo–thermal conversion applications. Composites Part B: Engineering 2021, 217, 108902.
[119] Nguyen, V.–T.; Min, B. K.; Yi, Y.; Kim, S. J.; Choi, C.–G., MXene($Ti_3C_2T_X$)/graphene/PDMS composites for multifunctional broadband electromagnetic interference shielding skins. Chemical Engineering Journal 2020, 393, 124608.
[120] Wu, X.; Han, B.; Zhang, H.–B.; Xie, X.; Tu, T.; Zhang, Y.; Dai, Y.; Yang, R.; Yu, Z.–Z., Compressible, durable and conductive polydimethylsiloxane–coated MXene foams for high–performance electromagnetic interference shielding. Chemical Engineering Journal 2020, 381, 122622.
[121] Wang, L.; Qiu, H.; Song, P.; Zhang, Y.; Lu, Y.; Liang, C.; Kong, J.; Chen, L.; Gu, J., 3D $Ti_3C_2T_x$ MXene/C hybrid foam/epoxy nanocomposites with superior electromagnetic interference shielding performances and robust mechanical properties. Composites Part A: Applied Science and Manufacturing 2019, 123, 293–300.
[122] Fan, Z.; Wang, Y.; Xie, Z.; Wang, D.; Yuan, Y.; Kang, H.; Su, B.; Cheng, Z.; Liu, Y., Modified MXene/holey graphene films for advanced supercapacitor electrodes with superior energy storage. Advanced Science 2018, 5, 1800750.
[123] Cheng, Y.; Li, X.; Qin, Y.; Fang, Y.; Liu, G.; Wang, Z.; Matz, J.; Dong, P.; Shen, J.; Ye, M., Hierarchically porous polyimide/$Ti_3C_2T_x$ film with stable electromagnetic interference shielding after resisting harsh conditions. Science advances 2021, 7, eabj1663.
[124] Cao, W.–T.; Chen, F.–F.; Zhu, Y.–J.; Zhang, Y.–G.; Jiang, Y.–Y.; Ma, M.–G.; Chen, F., Binary strengthening and toughening of MXene/cellulose nanofiber composite paper with nacre–inspired structure and superior electromagnetic interference shielding properties. Acs Nano 2018, 12, 4583–4593.
[125] Song, P.; Qiu, H.; Wang, L.; Liu, X.; Zhang, Y.; Zhang, J.; Kong, J.; Gu, J., Honeycomb structural rGO–MXene/epoxy nanocomposites for superior electromagnetic interference shielding performance. Sustainable Materials and Technologies 2020, 24, e00153.


ISSN 1584 – 2665 (printed version); ISSN 2601 – 2332 (online); ISSN–L 1584 – 2665